View metadata, citation and similar papers at core.ac.uk

brought to you by CORE

provided by Ghent University Academic Bibliography

Journal of Physics: Conference Series

PAPER • OPEN ACCESS

Trap-assisted tunnelling and Shockley-Read-Hall lifetime of extended defects in $In_{.53}Ga_{.47}As$ p+n junction

To cite this article: P C (Brent) Hsu *et al* 2019 *J. Phys.: Conf. Ser.* **1190** 012014

View the article online for updates and enhancements.

IOP ebooks™

Bringing you innovative digital publishing with leading voices to create your essential collection of books in STEM research.

Start exploring the collection - download the first chapter of every title for free.

This content was downloaded from IP address 134.58.253.30 on 15/06/2019 at 10:34

IOP Conf. Series: Journal of Physics: Conf. Series **1190** (2019) 012014 doi:10.1088/1742-6596/1190/1/012014

Trap-assisted tunnelling and Shockley-Read-Hall lifetime of extended defects in $In_{.53}Ga_{.47}As$ p+n junction

P C (Brent) Hsu[1,2], E Simoen[1,3], G Eneman[1], C Merckling[1], A Alian[1], R Langer[1], N Collaert[1] and M Heyns[1,2]

[1] IMEC, Kapeldreef 75, 3001 Leuven, Belgium
[2] KU Leuven, Department of Materials Engineering, 3001 Leuven, Belgium
[3] Ghent University, Department of Solid State Sciences, 9000 Gent, Belgium

Email: Brent.Hsu.ext@imec.be

Abstract. Several $In_{.53}Ga_{.47}As$ p+n junctions with various extended defect densities (EDDs) have been grown by metalorganic vapor phase epitaxy (MOVPE), by carefully controlling the growth conditions. After fabrication, T-dependent J-V, C-V and double DLTS (DDLTS) are performed to extract the electrical field dependence of the extended defect levels. From this characterization, it is derived that the extended defects dominate the electrical field enhancement factor Γ regardless of the value of the EDD and significantly increases the leakage current under reverse bias (i.e., decrease the Shockley-Read-Hall lifetime). These impacts are strongly connected to a "band-like" density of states of extended defects E2 at E_C-0.32 eV by comparing the DDLTS and T-dependent J-V characteristics. On the other hand, the reference sample (without EDs) surprisingly exhibits an even stronger field dependence with lower leakage current. Nevertheless, no straightforward candidate point defects can be found in this sample and the possible explanation are discussed.

1. Introduction

High saturation velocity and electron mobility make $In_{.53}Ga_{.47}As$ ternary alloys promising materials for several applications like high electron mobility transistors (HEMTs). Meanwhile, increasing the functionality of silicon CMOS and cost-reduction strongly push the integration of III-V alloy based devices on a silicon substrate. Although the growth of $In_{.53}Ga_{.47}As$ on silicon can be achieved by using different methods[1], it inevitably leads to extended defects during the heteroepitaxial growth. As a result, understanding the impacts of these crystalline defects on the electrical device performance and reliability is key to their successful development and integration on silicon substrates.

Deep level traps are well-known to degrade the device performance by forming efficient generation and recombination centers within the forbidden energy band. Besides, the effects of the electrical field such as trap-assisted tunneling (TAT) and Poole-Frenkel (PF) on these deep level traps enhance the carrier generation by tunneling or potential barrier lowering. In the case of dislocations, the impacts are amplified and more complicated due to the presence of a one-dimensional density of states (1D-DOS) along the dislocation line. So far, people are still struggling to reconstruct this 1D-DOS for different defects of various materials, and the interaction between the external electrical field and the internal electrical field by the charged dislocation core states is still unclear, motivating the study of the connection between extended defects and the electrical field dependence in the $In_xGa_{1-x}As$ ternary system.

Content from this work may be used under the terms of the Creative Commons Attribution 3.0 licence. Any further distribution of this work must maintain attribution to the author(s) and the title of the work, journal citation and DOI.
Published under licence by IOP Publishing Ltd

2. Sample preparation

Four p+/n-/n+ samples were grown on top of 2-inch semi-insulating InP(001) by metalorganic vapor phase epitaxy (MOVPE). The dopant element, thickness and doping density determined by SIMS and capacitance-voltage (C-V) profile are shown on Fig.1. The In content of the n+ layer was varied intentionally from 0.53 to 0.13 to create lattice-mismatch with the subsequent p+/n- $In_{.53}Ga_{.47}As$ junction. By introducing lattice mismatch, the different thermal expansion and hetero-epitaxy will form extended defects (EDs) to release the strain of layers.

The dominant extended defects are α and β 60° mixed misfit dislocations accompanied by a large number of stacking-faults, which could be observed by AFM, electron channeling contrast imaging (ECCI) and TEM (not shown here). The extended defect densities (EDDs) increase gradually along with the larger lattice-mismatch, giving the values of 10^5, 5×10^7, 2×10^8 and 9×10^9 cm^{-2} in the samples of x equal to 0.53, 0.47, 0.40 and 0.13, respectively (denoted as In53, In47, In40 and In13).

In order to apply electrical characterization, a top-top self-aligned contact fabrication was performed on all samples. A schematic structure is shown in Fig.1. The depletion depth at a reverse bias of 5 V is within the growth layer thickness (up to 600 nm from the junction), so that the detected region is only within the n- $In_{.53}Ga_{.47}As$ layer of interest.

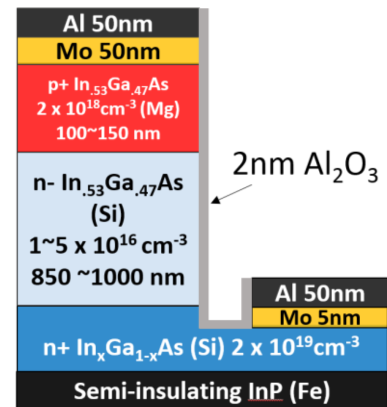

Figure 1. Schematic cross section of the junction diode (no scaling) after top-top self-aligned contact fabrication.

3. Experimental details

Current-Voltage (I-V) measurements were performed on a large set of diodes with the diameter of the circular junctions between 30 and 600 µm. The area leakage current density J_A is separated from the perimeter leakage current density J_P by plotting $\frac{I_{total}(V_R,T)}{P} = J_P(V_R,T) + \frac{A}{P}J_A(V_R,T)$ for different A/P ratio at fixed reverse bias and temperature, assuming a negligible corner and parasitic leakage current.

To further estimate the electrical field enhancement factor, C-V measurements at 1 MHz have been employed to determine the depletion depth W_R from $\varepsilon_{InGaAs}A/C_j$, where ε_{InGaAs} is the permittivity of $In_{.53}Ga_{.47}As$, A is the diode area and C_j is the junction capacitance. By combining J_A-V_R and W_R-V_R plots, a J_R versus W_R graph can be generated. Taking the derivative $\partial J_A/\partial W_R$ yields the generation lifetimes $\tau_g(W_R)$ from $qn_i/2\tau_g$ under large reverse bias (V_R>1 V), where q is the elementary charge and n_i is the intrinsic carrier concentration.

On the other hand, the generation lifetime under nearly zero bias electrical field $\tau_{g,F=0}$ was derived from small forward bias (V_F<0.5 V). By using full the expression $J_F = (J_{dA} + \frac{qn_iW_A}{2\tau_r \exp\left(\frac{qV}{2kT}\right)+\tau_g})(e^{qV/kT} - 1)$ and extrapolating τ_g from the qn_iW_A/J_{rbA0} versus $e^{qV/2kT}$ plots[2], one can yield another generation lifetime excluding the bias effect.

Finally, the electrical field enhancement factor Γ described by the Hurkx model[3] can be derived from plotting $\tau_{g,TAT}(W_R)^{-1} = [1 + \Gamma(W_R)]\tau_{g,SRH,F=0}$, versus the local maximum electrical field at each bias $F_{max} = \frac{qN_{dop}W_R}{\varepsilon_{InGaAs}}$, where N_{dop} is measured from a $1/C_j^2$ versus V_R plot.

4. Results and discussion

According to the J_A-V_R plot on Fig.2, a six orders of magnitude non-linear increase of the area leakage current density with increasing EDD can be observed, proving the existence of EDs has significant impacts on the studied p+n junctions. In addition, the slopes of $\partial J_A/\partial V_R$ change with reverse bias, giving that the generation lifetime is also in function of the reverse bias, which can be related to the local maximum electrical field F_{max}, assuming the ED and dominant point defects are uniformly distributed in the n- $In_{.53}Ga_{.47}As$ layer.

So, the next step is to examine the field enhancement factor Γ in function of the local maximum field F_{max} (Fig.3), presenting all the samples exhibit electrical field dependent generation current. It also shows that the sample In53, which is lattice-matched for all layers and expected to be dominated by point defects, displays a stronger field dependence than the other samples. Another important finding is that with the presence of EDs, the electrical field enhancement factor becomes consistent regardless of the change of EDDs. It indicates a similar mechanism/dependence for an EDD in the 5×10^6 to 8×10^9 cm^{-2} range. Because all of the samples have the same In content, doping density and almost no strain left (not shown here) in the n- layer of interest, the only change is the introduction of EDs by the lattice-mismatch. As a result, based on Fig.2 and Fig.3, the EDs not only cause an increasing of the leakage current but also dominate its electrical field dependence. The first impact will be discussed in another paper, here we will focus only on the field dependence of EDs.

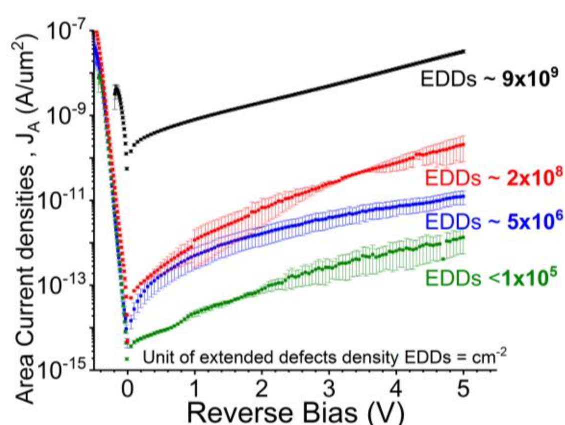

Figure 2. Area current density versus reverse bias with varying EDDs.

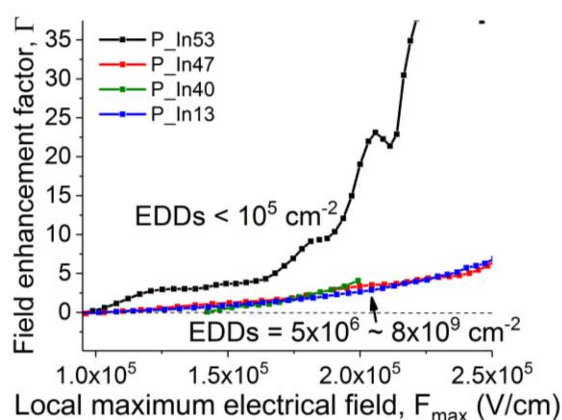

Figure 3. The field enhancement factor Γ versus local maximum electrical field with varying EDDs.

To further investigate the field dependence of EDs, the lattice-matched sample In53 (named defect-lean sample) and the highest lattice-mismatch sample In13 (named defective sample) have been chosen to perform Double-DLTS (DDLTS)[4] and temperature dependent current-voltage (T dependent J-V). These two techniques can give different electrical parameters under a fixed reverse bias, i.e., a constant electrical field: for DDLTS, by selecting different double pulse voltages, the trap parameter (activation energy ΔE_T and capture cross section σ) while "majority carriers emit from all possible traps" can be derived; for T-dependent J-V, by extracting Arrhenius plots under the same reverse bias, one can obtain the "dominant e^--h pair generation centers", which shouldn't be larger than the most efficient generation center located at mid-bandgap position. Note that the dominant generation center is not necessary the same as the deep level activation energies found in DDLTS.

The activation energies derived from T-dependent J-V (Fig.4) clearly show that the dominant generation center of the defective sample changes from mid-bandgap (ΔE_T ~0.37 eV) to a shallower position (ΔE_T ~0.17 eV) when the reverse bias increases, leading to the same conclusion, i.e., the defective sample exhibits a field dependence so that the effective activation energy becomes lower when F_{max} increases. On the other hand, the defect-lean sample exhibits a higher activation energy than mid-bandgap under smaller reverse bias (V_R<1.5 V), which can be explained by the dominance of the diffusion current. Because the diffusion current increases with the intrinsic carrier concentration squared, i.e., according to n_i^2, it will present an activation energy close to the bandgap of $In_{.53}Ga_{.47}As$.

From DDLTS of the defect-less lean sample (Fig.5), an electron trap PD1 located at E_C-0.16 eV is detected and identified as point defects by filling time measurements (not shown here). When changing the double pulse bias, no peak shift of PD1 is observed, i.e. no change of the activation energy ΔE_T, giving no field dependence when PD1 emits electrons to the conduction band. The reason

why F-dependence was found in Fig.3 but not in Fig.5 is still unclear. The possible explanation can be that either PD1 is not the dominant generation center, or the field dependence of PD1 is on the side of minority carriers (hole).

For the defective sample (Fig.6), "localized" states E1 at E_C-0.17 eV and "band-like" states E2 at E_C-0.32 eV under a filling pulse time of 500 µs were distinguished also by filling time measurement[5] (not shown here); a more detailed analysis will be reported in another paper. When changing the double bias from large reverse bias (larger F_{max}) to small V_R (smaller F_{max}), no peak shift is found for E1 but a shift to low temperatures for E2 is observed, which gives an activation shift from Ec-0.32 eV to a shallower level at Ec-0.15 eV. This activation energy shift coincides with the shift derived from Fig.4, reaching the conclusion that the dominant generation center most likely corresponds to E2. Note except the TAT or PF effect on the levels of band-like states E2, an alternative explanation is existence of the 1D-DOS of E2. Shallower levels of states on the edge of depletion will be filled when increasing pulse amplitude, which giving a higher band bending from junction, and cause a peak shift to low temperature of mean activation energy. (Similar as the DLTS measurement on density of interface of M-I-S structure)

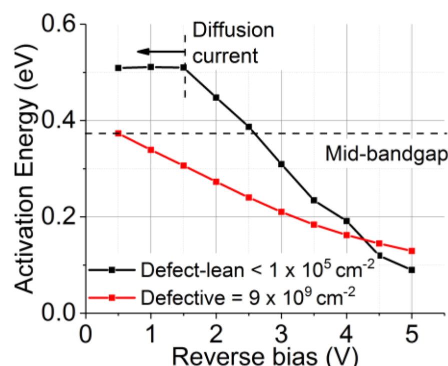

Figure 4. The activation energies derived from Arrhenius plots of T-dependent J_A-V_R graph under a fixed reverse bias.

In conclusion, the presence of EDs strongly increases the dark current under reverse bias. In addition, it governs the F-dependence with a consistent enhancement factor Γ, irrespective of the density for EDD ≥ 5×10^6 cm^{-2}. These effects are corresponding to a "band-like" density of states E2 located at Ec-0.32 eV under a filling pulse of 500 µs. So far, we connect E2 to stacking faults but more detailed characterizations are still needed. For the defect-lean sample, no straightforward connection between PD1 and the F-dependence has been derived, requiring further studies.

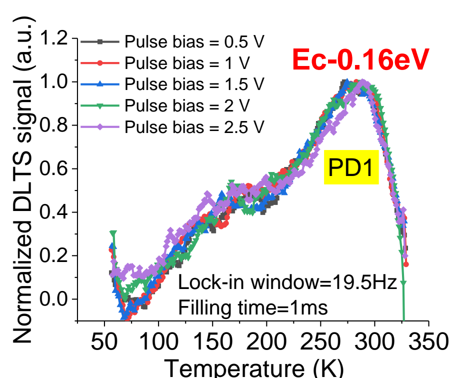

Figure 5. DDLTS of defect-lean sample, PD1 is a point defect at E_C-0.16eV.

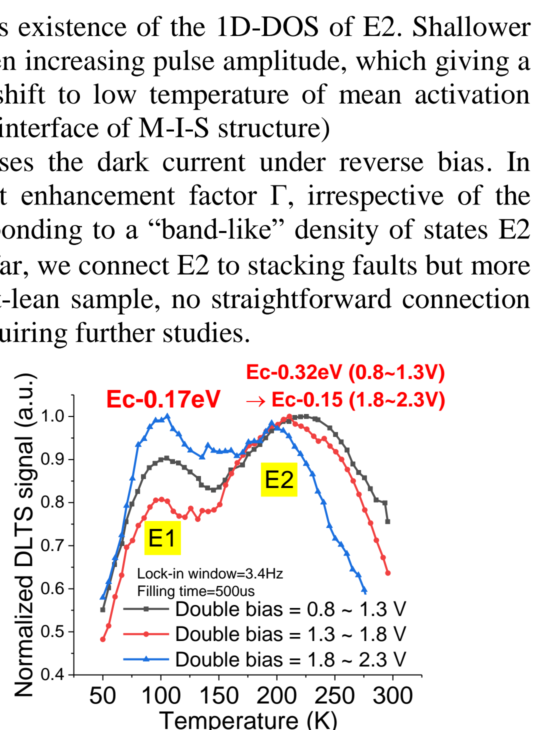

Figure 6. DDLTS of defective sample, E1 and E2 are "localized" and "band-like" states of EDs

References

[1] N. Collaert, "High Mobility Materials for CMOS Applications", ISBN: 9780081020623, (2018)
[2] A. Poyai, E. Simoen, C. Claeys, E. Gaubas, A. Huber, D. Gräf, *Materials Science and Engineering: B*, **B102,** 189-192, (2003)
[3] G. A. M. Hurkx, D. B. M. Klaassen, and M. P. G. Knuvers, *IEEE Trans. Electron Devices*, vol. **39**, no. 2, pp. 331–338, (1992)
[4] H. Lefèvre, and M. Schulz, *Appl. Phys.* **12**, 45-53, (1977)
[5] W. Schröter, J. Kronewitz, U. Gnauert, F. Riedel, and M. Seibt, *Phys. Rev. B* **52**, 13726, (1995)